Clay Minerals, (2016) **51**, 19–27

Effective removal of anionic and cationic dyes by kaolinite and TiO_2/kaolinite composites

W. HAJJAJI[1,2,*], S. ANDREJKOVIČOVÁ[1], R.C. PULLAR[3], D.M. TOBALDI[3], A. LOPEZ-GALINDO[4], F. JAMMOUSI[5], F. ROCHA[1] AND J.A. LABRINCHA[3]

[1] *Geobiotec, Geosciences Dept, University of Aveiro, 3810-193 Aveiro, Portugal*
[2] *Natural Water Treatment Laboratory, CERTE, 273, 8020 Soliman, Tunisia*
[3] *Department of Materials and Ceramic Engineering / CICECO, University of Aveiro, Aveiro, 3810-193, Portugal*
[4] *Instituto Andaluz de Ciencias de la Tierra, IACT-CSIC-UGR, Avda. Fuentenueva s/n, 18002, Granada, Spain*
[5] *Georesources Laboratory, Water Researches and Technology Center (CERTE), Borj Cedria Ecopark, BP 273, 8020 Soliman, Tunisia*

(*Received 1 October 2015; revised 4 February 2016; Editor: George Christidis*)

ABSTRACT: The present study investigated the removal of methylene blue (MB) and orange II (OII) dyes from synthetic wastewater by means of adsorption and photocatalysis using natural kaolins. For MB adsorption, the raw kaolinite-rich samples showed the greatest adsorption capacity, with rapid uptake (90% after 20 min). The experimental results were fitted better using the Langmuir isotherm model parameters compared to the Freundlich model, suggesting that the adsorption corresponds to monolayer coverage of MB molecules over the kaolinite surface. For OII, neither the Langmuir nor the Freundlich model gave reliable results, because the adsorption of anionic dye molecules by the clayey particles is not favoured.

Mixtures of kaolinite/Degussa TiO_2 were also prepared, and their photocatalytic properties under UV-light exposure were investigated. Decolourization of MB solutions was observed, even in a mixture with low TiO_2 content. This is related to the combined effect of adsorption and photocatalysis and, unlike the pure clay samples, the efficiency of such mixtures against OII was only slightly weaker (80–94%).

For TiO_2-impregnated clays, with the kaolinite layers separated by sol-gel TiO_2 particles, the MB removal was slow and effective only after >24 h due to the complexity of the bonding of MB molecules. On the other hand, the removal performance against OII solutions was very efficient (nearly 100%) within only 2 h. This excellent performance was attributed to morphological changes in clay particles.

KEYWORDS: kaolinite, TiO_2, dyes, adsorption, photocatalysis.

Because of their many useful properties (*e.g.* porosity, plasticity, inertness), clay minerals are currently being investigated as attractive, low-cost materials for waste treatment. With the ever-increasing growth in manufacturing and consumption, the problems caused by industrial wastes and wastewater have become a major issue. Dyes are common pollutants from many different industries, ranging from textiles to pharmaceutical plants (Hunger, 2002). They pose serious environmental and health hazards to both humans and aquatic and marine ecosystems (Christie, 2007; Gupta & Suhas, 2009). Their removal from industrial effluents before discharge into the environment is of paramount importance because of their toxicity and possible accumulation in the environment. Among the various techniques to remove dyes from effluents, adsorption,

*E-mail: w.hajjaji@ua.pt
DOI: 10.1180/claymin.2016.051.1.02

coagulation, oxidation and biosorption have been investigated and developed extensively (Slokar & Majcen-Le Marechal, 1998; Robinson *et al.,* 2001; Aksu, 2005; Ali & Gupta, 2007; Wang *et al.,* 2008). In the field of adsorption, recent efforts concern the use of new and low-cost sorbents. Clays (bentonite, kaolin, sepiolite), zeolites and lime have been used successfully as alternative materials (Gupta & Suhas, 2009).

These minerals, which are abundant in Portugal, have been reported as good adsorbents in various publications (Santos *et al.,* 2006; Quintelas *et al.,* 2011). Due to their layer or tubular structure, they have large specific surface areas and adequate mechanical and chemical stability. Among them, untreated montmorillonite and bentonite (Eren & Afsin, 2008; Gupta & Suhas, 2009), sepiolite (Ozcan *et al.,* 2006), palygorskite (Al-Futaisi *et al.,* 2007), kaolinite (Gupta & Suhas, 2009) and zeolite (Wang *et al.,* 2006) are the most widely exploited minerals. Another material used for the removal of dyes is titania (TiO_2) *via* a photocatalytic reaction (Fujishima *et al.,* 2008). This method is considered as very efficient and environmentally safe for wastewater treatment. The ability of TiO_2 to oxidize chemical compounds is exploited to decompose or mineralize organic pollutants (Fujishima *et al.,* 2000; Hermann *et al.,* 2007). Detoxification of various harmful compounds in both water and air has been demonstrated, using TiO_2 powder, to purify wastewater and polluted air (Carp *et al.,* 2004; Fujishima *et al.,* 2008). Among the semiconductor photocatalysts, TiO_2 is the most widely studied and used in many applications, because it has a strong oxidation ability, is known to have superhydrophilic properties, is chemically stable in acidic and alkaline media, and is non-toxic, commercially available and inexpensive (Fujishima *et al.,* 2000, 2008). Recent research about clays and other low-cost materials for waste treatment, both with and without additions of TiO_2 has included work by Liu *et al.* (2009) and Chong *et al.* (2009), for TiO_2/montmorillonite and TiO_2/kaolinite, respectively.

In the present study, the ability of two kaolinites (a natural kaolinite from Portuguese deposits and a commercial one) to absorb a cationic dye (methylene blue, MB) and an anionic dye (orange II, OII) was tested. The clays were also used as substrates for TiO_2 (Chong *et al.*, 2009). The kaolinite/TiO_2 was produced in two ways: by the simple mixture of TiO_2 nanopowder and kaolinite in different proportions, and by the drop-wise addition of an aqueous TiO_2 sol. The final products were then tested as photocatalysts for the degradation of MB and OII.

MATERIALS AND METHODS

The present study investigated the removal of MB and OII dyes (both obtained from from Sigma-Aldrich) from synthetic wastewater by adsorption and photocatalysis with two natural kaolinitic clays. K1 is a representative Portuguese natural clay and K2 is a commercial kaolin (VWR Prolabo, Belgium). The full characterization of the clays will be presented in the following section.

The mineralogical composition of the bulk and clay fractions were determined by X-ray diffraction (XRD) using a Philips X'Pert diffractometer with CuKα radiation. The traditional methodology for clay determination of oriented aggregates was followed (Moore & Reynolds, 1989), including treatment with ethylene-glycol and heating to 550°C. For mineral quantification, we combined the measurements of peak areas in diffraction patterns (Zevin & Kimmel, 1995) and chemical data (López-Galindo *et al.,* 1996). The experimental error is ±5%. The microstructural characterization was carried out by scanning electron microscopy (SEM – Hitachi, SU 70) and energy dispersive X-ray analysis (EDS-EDAX with a Bruker AXS detector and Quantax software). Chemical analysis was carried out by X-ray fluorescence (XRF) spectrometry using an Axios Wavelength Dispersive XRF spectrometer. Loss on ignition (LOI) was estimated by measuring the difference in weight between a dried 10 g sample and one calcined at 1000°C. The specific surface areas of the clays were determined by the BET method (Brunauer *et al.,* 1938) with nitrogen gas adsorption at 77 K. The adsorption/desorption isotherms were obtained by the same apparatus. The microstructural characterization was conducted by scanning electron microscopy (SEM-Hitachi, SU 70).

For the dye-adsorption measurements, a given amount of K1 or K2 kaolin was dispersed in 100 mL of dye aqueous solutions at pH = 7, containing varying amounts of dye (50, 75, 100, 125, 150 and 200 ppm). The dispersions were then stirred at 200 rpm at 20°C for a given time (t = 0, 10, 20, 40, 60 and 120 min).

Two different methods were used to add TiO_2 to the clays for photocatalytic testing. In the first, different ratios of a commercial TiO_2 nanopowder (Degussa P25, now renamed Aeroxide P25) were added to the clay (K1 or K2). The ratios used were: 100 wt.% Degussa TiO_2 (T100K0), 80/20 wt.% TiO_2/clay (T80K20), 60/40 wt.% (T60K40), 50/50 wt.% (T50K50), 40/60 wt.% (T40K60) and 20/80 wt.% (T20K80). P25 has a particle size of 21 nm, and is known to consist of 78 wt.%

Table 1. XRD and XRF quantification.

Mineralogy (%)										
	Kaolinite	Illite	Illite-Smectite		Quartz	Feldspar	Calcite			
K1	45	8	–		39	8	–			
K2	73	8	7		7	3	2			
Chemical analysis (wt.%)										
	SiO_2	Al_2O_3	Fe_2O_3	MgO	CaO	Na_2O	K_2O	TiO_2	P_2O_5	LOI
K1	70.07	21.17	0.96	0.39	0.03	0.10	1.86	0.76	0.03	4.63
K2	49.29	34.84	1.11	0.32	0.40	–	1.76	0.41	–	11.75

anatase, 14 wt.% rutile and 8 wt.% amorphous matter (Ohtani *et al.,* 2010). In the second method an aqueous TiO_2 sol was prepared using the method published previously by the authors (Tobaldi *et al.,* 2013a), prepared as a Ti^{IV} sol with a concentration of 1 mol L^{-1}. 2.4 mL of this sol was added dropwise to an aqueous suspension of 0.5 g of each clayey sample (K1 or K2). This was equivalent to 0.192 g of TiO_2, yielding a sample with ~72 wt.% clay and 28 wt.% TiO_2. The resulting suspension was washed with deionized water, and heated at 80°C to obtain the final TiO_2-impregnated powder. The sol particles were 10 nm, and when heated to 80°C, the TiO_2 sol consisted of 43.4 wt.% anatase, 13.3% rutile, 13.1 wt.% brookite and 30.2% amorphous matter (Tobaldi *et al.,* 2013b). The unit-cell parameters of anatase and rutile in the heated sol were determined with Rietveld refinement.

The photocatalysis tests were performed at room temperature, in a 0.5 L cylindrical photocatalytic reactor containing an aqueous solution of the dye with initial concentration 10 mg L^{-1}. The concentration of the TiO_2-modified-kaolin photocatalyst in the slurry was 0.25 g L^{-1}. The suspension (TiO_2 + clay + dye) was stirred in the dark for 30 min, to allow the adsorption/desorption of MB and OII onto the powders. The lighting of the reacting system was assured by placing two lamps at either side of the reactor; the distance between the lamps and the reactor was 5 cm. The UVA-light source was a germicidal lamp (Philips PL-S 9W, NL), with an irradiance of ~13 W m^{-2} in the UVA range. The photocatalytic degradation of MB and OII was monitored by sampling ~4 mL of the slurry from the reactor, at regular time intervals. The collected solution samples were centrifuged and the residual concentration of MB and OII monitored by UV-visible spectrophotometry (Shimadzu UV 3100) at 665 and 486 nm, respectively.

The extent of MB photocatalytic degradation, ξ, was evaluated from the following equation:

$$\xi\% = \frac{C_0 - C_s}{C_0} \times 100$$

where C_0 is the initial dye concentration and C_S is the concentration after a certain UVA irradiation time. Based on duplicate and in some cases triplicate experiments, the standard error was estimated to be <5%.

RESULTS AND DISCUSSION

Kaolin characterization

The quantitative mineralogical composition based on XRD (wt.%) is reported in Table 1. The Portuguese kaolin (K1) is composed of 45% kaolinite, 8% illite, 39% quartz and 8% feldspars. A larger amount of kaolinite (73%) and a smaller proportion of quartz (7%) was determined in the commercial kaolin (K2), in accordance with the lesser abundance of SiO_2 and the greater abundance of Al_2O_3. K2 also contains 7% interstratified illite/smectite (Ill/Sm).

The K1 and K2 kaolins display a small surface area (~18 m^2 g^{-1}) due to the dominance of kaolinite. The monolayer interaction between adsorbent and adsorbate was fitted with Type II adsorption isotherms (Brunauer *et al.,* 1938) (Fig. 1). Assuming neutral pH (measured ~7), a smaller N_2 uptake close to the saturation pressure was observed for the commercial kaolin K2 (quasi-overlapping adsorption-desorption curves). The intersection of the desorption branch with

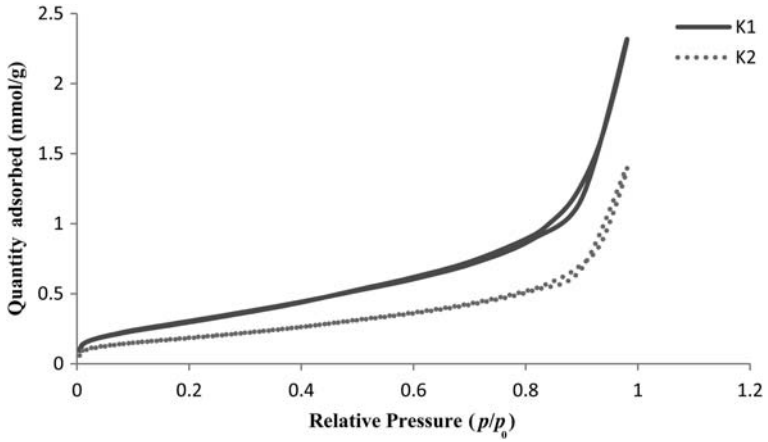

FIG. 1. Nitrogen adsorption and desorption isotherms: type IV adsorption isotherms of K1 and K2 kaolins.

the adsorption branch in K2 is attributed to experimental error.

Adsorption study

The kinetics of MB and OII dye adsorption were evaluated as a function of contact time and initial dye concentration, for the pure clays K1 and K2 (Fig. 2). Both samples have similar MB uptake behaviour, which exceeds 90% after just 20 min of contact time, and reach an optimum after 1 h, which is an equilibrium state with maximum adsorption (Fig. 2a). The capacity of the adsorbent was also studied with varying initial concentration (Fig. 2b). For MB concentrations up to 100 ppm, the uptake capacity of clays K1 and K2 exceeded 95%. At greater concentrations, the clayey materials reached their saturation point, and the adsorption of MB decreased rapidly with increasing dye concentration. This decrease was more accentuated in the case of K1 (only 43% MB was adsorbed with 200 ppm as the initial concentration), because of the smaller proportion of phyllosilicates (53%) in comparison with K2, which has a greater clay-minerals content (88%). For OII (Fig. 2), the adsorption rate was small due to the anionic nature of this dye (<10%). The uptake of negatively charged

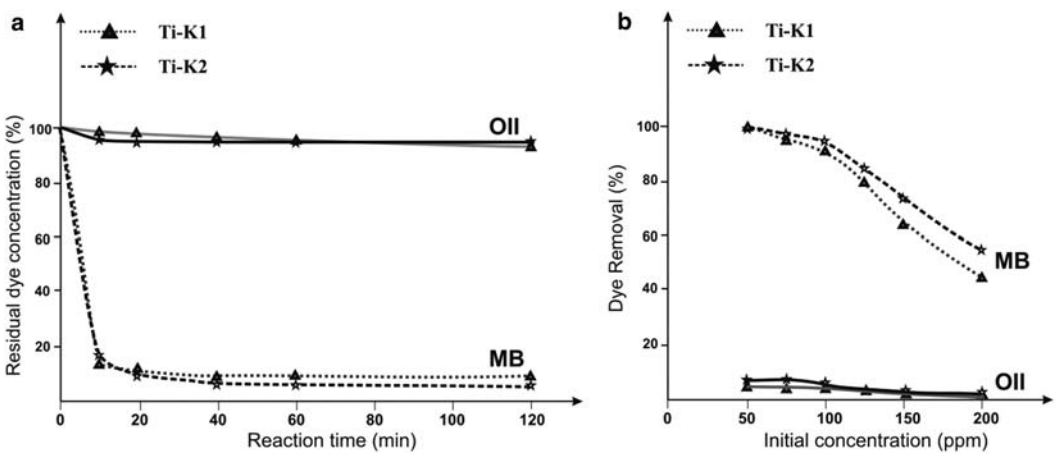

FIG. 2. Adsorption kinetics: (a) residual dye concentration with contact time for an initial dye concentration of 10 ppm; and (b) % dye removal with initial dye concentration after a reaction time of 1 h, for MB and OII dyes, for the pure clays K1 and K2.

TABLE 2. Adsorption isotherm parameters for methylene blue (MB) and Orange II (OII).

Samples	Langmuir equation					Freundlich equation			
	MB				OII	MB			OII
	Q_m	K_L	R_L	R^2	R^2	K_f	n	R^2	R^2
K1	22.2	0.0026	0.021	0.950	0.03	1.5	2.290	0.927	0.01
K2	23.1	0.0013	0.010	0.988	0.01	2.15	1.406	0.979	0.01

molecules by the non-activated clays is extremely limited.

The MB adsorption isotherm model parameters fit better with the Langmuir model, with greater R^2 values of 0.950 and 0.988 for K1 and K2, respectively (Table 2). In this case, the monolayer adsorption process is highly favoured in both samples. The adsorption capacity, Q_m, of these clays, estimated from the Langmuir monolayer model (22.2 and 23.1 mg g^{-1}), is close to the experimental data obtained (~18 mg g^{-1} measured by BET), due to the kaolinitic nature of the samples (>60% kaolinite). Following the Freundlich model (Table 2), the n factor showed a favourable MB adsorption process ($n > 1$), and considering that $0 < 1/n < 1$, there were increased probabilities of multilayer adsorption. For OII, the application of both Langmuir and Freundlich models are inappropriate because of the low adsorption profiles (low R^2 values).

Photocatalysis measurements

Photocatalysis measurements were carried out on the TiO_2-modified clays, with additions of either P25 or the TiO_2 sol. The photodegradation of MB and OII by different ratios of clay/P25 TiO_2 is shown in Table 3, where the MB removal efficiency (ξ) is the % of MB removed after 5 h. Better MB removal efficiency (ξ) is observed in K2 mixtures (up to 94%). This is attributed to the smaller amount of

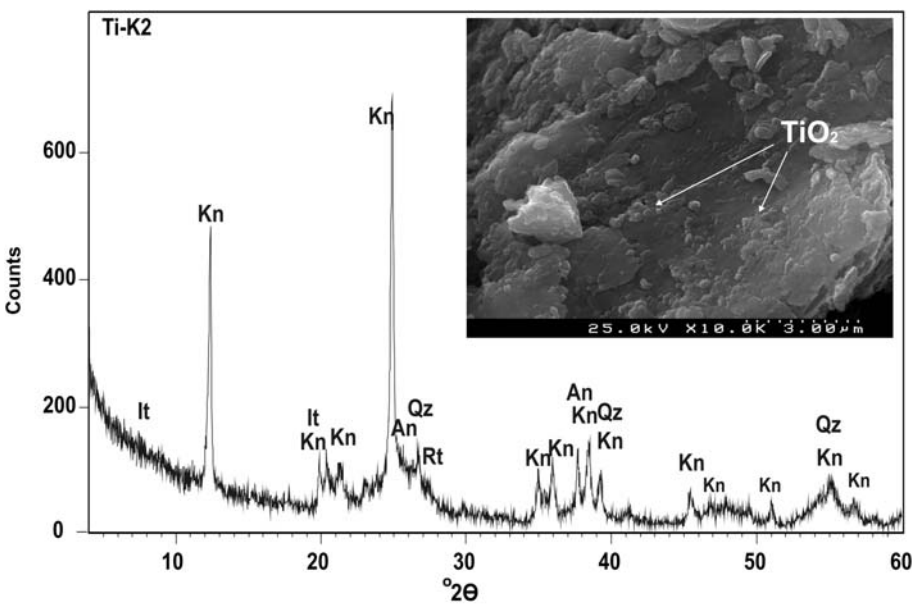

FIG. 3. SEM image and XRD pattern of TiO_2-impregnated Ti-K2 clay. Kn: kaolinite, An: anatase, Rt: rutile, It: illite, and Qz: quartz.

Table 3 Photodegradation efficiency (ξ) and coefficient of determination (R^2).

		100T0K		80T20K		60T40K		50T50K		40T60K		20T80K	
		ξ (%)	R^2	ξ (%)	R^2	ξ (%)	R^2	ξ (%)	R^2	ξ (%)	R^2	ξ (%)	R^2
K1	MB	99	0.96	92	0.93	98	0.81	94	0.72	95	0.78	78	0.25
	OII	96	0.94	90	0.91	86	0.92	84	0.93	80	0.93	61	0.93
K2	MB	99	0.96	98	0.97	99	0.98	96	0.9	97	0.9	94	0.61
	OII	96	0.94	93	0.92	92	0.92	96	0.94	99	0.94	83	0.97

phyllosilicates in K1, which might lead to fewer active adsorptive and photocatalytic sites for the degradation of organic molecules. On the other hand, the two clays containing only 40 wt.% of Degussa TiO_2, displayed acceptable MB dye removal exceeding 92%, close to that achieved using 100% of the commercial TiO_2 photocatalyst (100T0 K). These results are explained by the combination of adsorption and photocatalysis efficiency of these clay mixtures with a minor amount of Degussa P25 TiO_2. This hypothesis is confirmed by the decrease in the coefficient of determination, R^2, with the amount of TiO_2 used (Table 3).

The degradation of OII by different TiO_2/clay mixtures shows values of R^2 superior to those related to MB photocatalytic mineralization. This behaviour was expected, because the influence of adsorption is practically absent due to the anionic nature of OII. The Degussa P25 sample with TiO_2 content of <40%, also showed a poorer removal efficiency. Nevertheless, the removal is within an acceptable range (>80% for both 40T60 K samples; Table 3).

The XRD pattern of the TiO_2-impregnated Ti-K2 clay is presented in Fig. 3. A poorly crystalline structure is present (broad band centred at 25°2θ), probably related to the incompletely crystallized TiO_2 when heated at 80°C (contains ~30 wt.% amorphous matter). The presence of anatase was demonstrated by the peak at 25.3°2θ (101), and rutile by that at 27.5°2θ (110). Quartz and illite are also present.

The SEM image confirmed the presence of TiO_2 nanoparticles on the kaolinite surface (Fig. 3). The TiO_2 particles are impregnated on platy kaolinite crystals.

The anatase unit-cell volume (Table 4) showed a contraction compared to that in *JCPDS* card 211272, while that of rutile showed an expansion compared to that of *JCPDS* card 211276. The dependence of the lattice-volume contraction/expansion on the reduction of the crystalline domain size is in accordance with the work of Li *et al.* (2005) and of Kuznetsov *et al.* (2009). The volume contraction of (nano)anatase is attributed to its highly hydrated surfaces (Li *et al.,* 2005). The (nano)rutile volume expansion has been ascribed to Ti vacancies (Kuznetsov *et al.,* 2009). Compared with P25 TiO_2 (anatase: a = 3.77 Å; c = 9.48 Å; rutile: a = 4.58 Å; b = 3.03 Å (Gao *et al.,* 2009)), the lattice parameters of the TiO_2 phases determined in the present study are smaller. This should result in small particle sizes leading to large surface areas providing more active sites (Lv *et al.,* 2009).

Figure 4 illustrates the photocatalytic kinetics of MB and OII by the TiO_2-impregnated Ti-K1 and Ti-K2 samples, compared to pure Degussa P25 TiO_2. After

Table 4. Anatase and rutile unit-cell parameters, as determined with Rietveld refinement of the titania gel, dried at 80°C, and unit-cell parameters of anatase and rutile from JCPD F cards 211272 and 211276, respectively.

	Anatase			Rutile		
	$a = b$ (Å)	c (Å)	Volume (Å^3)	$a = b$ (Å)	c (Å)	Volume (Å^3)
TiO_2 dried gel	3.7795(12)	9.4469(51)	134.94(9)	4.6166(4)	2.9583(5)	63.05(1)
JCPDF 211272	3.7852	9.5139	136.31			–
JCPDF 211276			–	4.5933	2.9592	62.43

The agreement factors of the refinement were: $R(^2_F)$ = 2.20%, R_{wp} = 5.23%, χ^2 = 1.60.

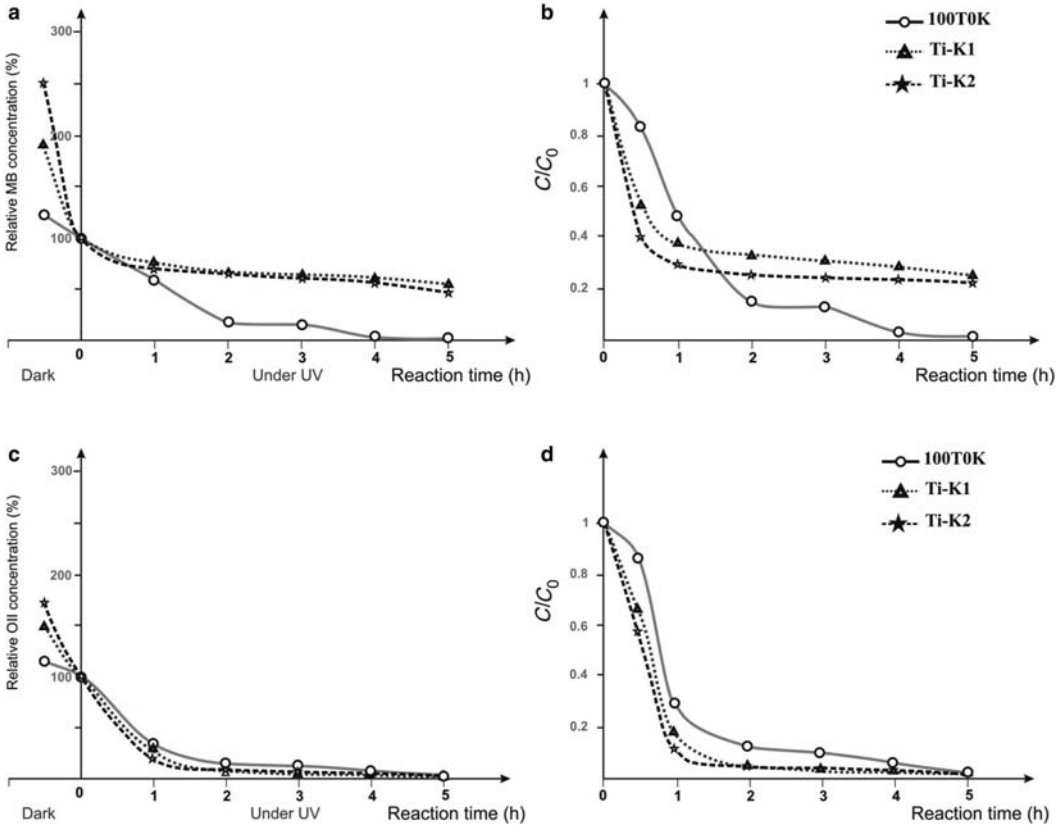

FIG. 4. Photocatalysis removal kinetics of MB (a,b) and OII (c,d) dyes by pure Degussa P25 titania, and by the titania-sol-modified clays Ti-K1 and Ti-K2. (a) and (c) show relative dye concentrations after adsorption has occurred in the dark for 30 min, normalized to 100% after this time; (b) and (d) show the absolute change in dye concentration with time.

exclusion of the adsorption effect that occurs during the first 30 min in the dark, the relative photocatalytic dye removal rates were normalized to 100% from the start of exposure to UV light (Fig. 4a,c). Figures 4b and 4d show the absolute total dye removal from the moment the clay/TiO_2 nanocomposite is added, and combines adsorption and photocatalytic processes.

A relatively weak degradation (<35%) of MB under UV light was noticed in both impregnated kaolinitic samples (Fig. 4a). This behaviour might result from the double benzene ring being bound in complex fashion to the bridging nitrogen in MB molecules, which is only partially broken even after 5 h; however this has yet to be proved. Only after 20 h of UV radiation was almost complete degradation of Ti-K1 and Ti-K2 observed. Despite this moderate photocatalytic activity, the TiO_2-impregnated clays showed reasonable MB removal, superior to the Degussa P25 TiO_2, during the first 90 min (Fig. 4b). Due to their greater adsorption capacities, they initially removed MB much faster than the P25, exceeding 40% removal after just 1 h, although for the most part this, was not due to photocatalysis. The removal mechanism was dominated by adsorption and led to a greater decrease in absolute dye concentration (C/C_0) in the case of Ti-K2, due to the greater phyllosilicate content.

Both Ti-K samples displayed fast removal and greater efficiency of degradation of OII (up to 99%) within a short time of 2 h, comparable to that of pure Degussa P25 TiO_2 (Fig. 4c). The light-activated removal of OII is almost identical to that of pure P25, despite the fact that the TiO_2-impregnated clays contain only 28% TiO_2, more than 50% of which is the UV-activated anatase phase. This superior activity is probably due to a better distribution of the nano-sized TiO_2 from the sol, and the porous nature of TiO_2-impregnated clays. However, in the case of OII (Fig. 4d), the TiO_2-sol-modified clays removed OII faster than P25, which reached almost 100%

after only 2 h, superior to the P25. Moreover, the TiO_2-impregnated clays have a superior adsorption rate of the anionic OII dye compared to the pure kaolin samples.

CONCLUSIONS

Two kaolinitic samples were tested for the removal of MB and OII dyes by adsorption and photocatalysis. Following adsorption, the clays showed MB removal exceeding 90% after just 20 min of contact time, and an optimum uptake (95%) for MB concentrations of <100 ppm. With OII, the adsorption rate was small (<10%) due to the anionic nature of this dye. The photodegradation of MB and OII using clays modified with TiO_2 was also investigated. The clays mixed with Degussa P25 titania displayed excellent MB-removal efficiencies (ξ), achieving at least 95% removal even with P25 levels as low as 40 wt.%, largely due to adsorption on the clay. Furthermore, high removal rates of >80% were also achieved with OII, which are related to the combined effects of adsorption and photocatalysis. When the TiO_2-sol-impregnated clays were tested, the photocatalytic MB degradation was much slower than that for pure P25 TiO_2 and was still incomplete even after 20 h. However, the removal of OII was superior to that achieved with pure P25 TiO_2, approaching 100% removal after only 2 h due to a combination of photocatalytic and adsorption processes.

ACKNOWLEDGEMENTS

The present work was supported by FCT-Grant SFRH/BPD/72398/2010 co-financed by Programa Operacional potencial Humano POPH. R.C. Pullar thanks the FCT Ciência2008 Programme for supporting this work. D.M. Tobaldi gratefully acknowledges FCT for financial support (grant BPD/UI89/5681/2012).

REFERENCES

Aksu Z. (2005) Application of biosorption for the removal of organic pollutants: a review. *Process Biochemistry*, **40**, 997–1026.

Al-Futaisi A., Jamrah A. & Al-Hanai R. (2007) Aspects of cationic dye molecule adsorption to palygorskite. *Desalination*, **214**, 327–342.

Ali I. & Gupta V.K. (2007) Advances in water treatment by adsorption technology. *Nature Protocols*, **1**, 2661–2667.

Brunauer S., Emmett P.H. & Teller, E.J. (1938) Adsorption of gases on multimolecular layers. *Journal of the American Chemical Society*, **60**, 309–319.

Carp O., Huisman C.L. & Reller A. (2004) Photoinduced reactivity of titanium dioxide. *Progress in Solid State Chemistry*, **32**, 33–177.

Chong M.N., Vimonses V., Lei S., Jin B., Chow C. & Saint C. (2009) Synthesis and characterisation of novel titania impregnated kaolinite nano-photocatalyst. *Microporous and Mesoporous Materials*, **117**, 233–242.

Christie R.M. (2007) *Environmental Aspects of Textile Dyeing.* Woodhead, Boca Raton, Florida, and Cambridge, UK.

Eren E. & Afsin B. (2008) Investigation of a basic dye adsorption from aqueous solution onto raw and pre-treated bentonite surfaces. *Dyes and Pigments*, **76**, 220–225.

Fujishima A., Rao T.N. & Tryk D.A. (2000) Titanium dioxide photocatalysis. *Journal of Photochemistry and Photobiology C: Photochemistry Reviews*, **1**, 1–21.

Fujishima A., Zhang X. & Tryk D.A. (2008) TiO_2 photocatalysis and related surface phenomena. *Surface Science Reports*, **63**, 515–582.

Gao X., Liu J. & Chen P. (2009) Nitrogen-doped titania photocatalysts induced by shock wave. *Materials Research Bulletin*, **44**, 1842–1845.

Gupta V.K. & Suhas (2009) Application of low-cost adsorbents for dye removal: a review. *Journal of Environmental Management*, **90**, 2313–2342.

Herrmann J.-M., Duchamp C., Karkmaz M., Hoai Bui Thu, Lachheb H., Puzenat E. & Guillard C. (2007) Environmental green chemistry as defined by photocatalysis. *Journal of Hazardous Materials*, **146**, 624–629.

Hunger K. (2002) *Industrial Dyes.* Chemistry Properties, Applications., Wiley-VCH, Weinheim, Germany.

Kuznetsov A.Y., Machado R., Gomes L.S., Achete C.A., Swamy V., Muddle B.C. & Prakapenka V. (2009) Size dependence of rutile TiO_2 lattice parameters determined via simultaneous size, strain, and shape modeling. *Applied Physics Letters,* **94,** 193117.

Li G., Li L., Boerio-Goates J. & Woodfield B.F. (2005) High purity anatase TiO_2 nanocrystals: Near room-temperature synthesis, grain growth kinetics, and surface hydration chemistry. *Journal of the American Chemical Society*, **127**, 8659–8666.

Liu J.J., Dong M.Q., Zuo S.L. & Yu Y.C. (2009) Solvothermal preparation of TiO_2/montmorillonite and photocatalytic activity. *Applied Clay Science*, **43**, 156–159.

Lopez-Galindo A., Torres-Ruis J. & Gonazlez-Lopez J.M. (1996) Mineral quantification in sepiolite-palygorskite deposits using X-ray diffraction and chemical data. *Clay Minerals*, **31**, 217–224.

Lv K., Zuo H., Sun J., Deng K., Liu S., Li X. & Wang D. (2009) (Bi, C and N) codoped TiO_2 nanoparticles. *Journal of Hazardous Materials*, **161**, 396–401.

Moore D.M. & Reynolds R.C. (1989) *X-ray diffraction and Identification and Analysis of Clay Minerals.* Oxford University Press, New York.

Ohtani B., Prieto-Mahaney O.O., Li D. & Abe R. (2010) What is Degussa (Evonik) P25? Crystalline composition analysis, reconstruction from isolated pure particles and photocatalytic activity test. *Journal of Photochemistry and Photobiology A: Chemistry*, **216**, 179–182.

Ozcan A., Oncu E.M. & Ozcan A.S. (2006) Kinetics, isotherm and thermodynamic studies of adsorption of Acid Blue 193 from aqueous solutions onto natural sepiolite. *Colloids and Surfaces A*, **277**, 90–97.

Quintelas C., Figueiredo H. & Tavares T. (2011) The effect of clay treatment on remediation of diethylketone contaminated wastewater: Uptake, equilibrium and kinetic studies. *Journal of Hazardous Materials*, **186**, 1241–1248.

Robinson T., McMullan G., Marchant R. & Nigam P. (2001) Remediation of dyes in textile effluent: a critical review on current treatment technologies with a proposed alternative. *Bioresource Technology*, **77**, 247–255.

Santos S.C.R., Boaventura R.A.R. & Oliveira Á.F.M. (2006) Preliminary study on the adsorption of the cationic dye Astrazon red by a Portuguese bentonite. Pp. 111–116 in: *Combined and Hybrid Adsorbents.* NATO Security through Science Series.

Slokar Y.M. & Majcen-Le Marechal A. (1998) Methods of decoloration of textile wastewaters. *Dyes and Pigments,* **37,** 335–356

Tobaldi D.M., Pullar R.C., Gualtieri A.F., Seabra M.P. & Labrincha J.A. (2013a) Sol-gel synthesis and characterisation of pure, W-, Ag-, and W/Ag co-doped TiO_2 nanopowders. *Chemical Engineering Journal*, **214**, 364–375.

Tobaldi D.M., Pullar R.C., Gualtieri A.F., Seabra M.P. & Labrincha J.A. (2013b) Phase composition, crystal structure and microstructure of silver and tungsten doped TiO_2 nanopowders, with tuneable photochromic behavior. *Acta Materialia*, **61**, 5571–5585.

Wang S., Li H., Xie S., Liu S. & Xu L. (2006) Physical and chemical regeneration of zeolitic adsorbents for dye removal in wastewater treatment. *Chemosphere*, **65**, 82–87.

Wang S., Ang H.M. & Tadé M.O. (2008) Novel applications of red mud as coagulant, adsorbent and catalyst for environmentally benign processes. *Chemosphere*, **72**, 1621–1635.

Zevin L.S. & Kimmel G. (1995) *Quantitative X-ray Diffractometry.* Springer, New York.